Ocean Modelling xxx (2010) xxx–xxx

Contents lists available at ScienceDirect

Ocean Modelling

journal homepage: www.elsevier.com/locate/ocemod

Development of the POLCOMS–WAM current–wave model

R. Bolaños [a,*], P. Osuna [b], J. Wolf [a], J. Monbaliu [c], A. Sanchez-Arcilla [d]

[a] National Oceanography Centre, Joseph Proudman Building, 6 Brownlow Street, Liverpool L3 5DA, UK
[b] Departamento de Oceanografía Física, División de Oceanología, CICESE, Carretera Tijuana-Ensenada No. 3918, Zona Playitas, 22860 Ensenada, B.C., Mexico
[c] Hydraulics Laboratory, Katholieke Universiteit Leuven, Kasteelpark Arenberg 40, Hervelee 3001, Belgium
[d] Laboratori d'Enginyeria Marítima, Universitat Politècnica de Catalunya, c/ Jordi Girona, 1-3, Campus Nord-UPC, Edif. D-1, 08034 Barcelona, Spain

A R T I C L E   I N F O

Article history:
Received 2 February 2010
Received in revised form 24 August 2010
Accepted 22 October 2010
Available online xxxx

Keywords:
Ocean modelling
POLCOMS
Wave modelling
WAM
Mediterranean
Ocean dynamics

A B S T R A C T

The continuous research and improvement of ocean modelling helps to provide a more sustainable development of coastal and offshore regions. This paper focuses on ocean modelling at the NW Mediterranean using the POLCOMS–WAM model with new developments. The Stokes' drift effect on currents has been included and the distribution of surface stress between waves and currents has also been considered. The system is evaluated in the NW Mediterranean and an evaluation of different forcing terms is performed. The temperature and salinity distributions control the main patterns of the Mediterranean circulation. Currents are typically small and therefore the modification of waves due to the effect of currents is minimal. However, the wave induced currents, mainly caused by a modified wind drag due to waves, produce changes that become an important source of mass transport. POLCOMS was able to reproduce the main Mediterranean features, its coupling with WAM can be a very useful tool for ocean and wave modelling in the Mediterranean and other shelf seas.

1. Introduction

Coastal waves and currents are highly variable and can have a significant impact on human activities and structures; increased utilisation of the marine environment for food, energy and other resources increases the need for understanding the marine system. There is also a need to understand the interactions of waves and currents in the near-shore zone as nonlinear effects become more important, waves contribute to the mean circulation and the latter modifies waves. The impact of waves and surges at the coast are closely linked (Wolf, 2009). The prediction of wind-waves and ocean currents is of great importance for the management (including navigation) of coastal areas. Therefore, the continuous research and improvement of operational forecasting and monitoring become vital issues for the safety and well-being of coastal society. The capability of monitoring and predicting the marine environment leads to a more sustainable development of coastal and offshore regions. In recent years operational oceanography has been considered a necessity given its essential role in solving economic, environmental and social problems (Pinardi and Woods, 2002). Ocean currents also control the renewal of shelf and coastal waters which is linked to water quality in coastal areas with the consequent impact on economics and tourism. Finally, a last example would be oil spill prediction, search and rescue operations. These activities mainly depend on the correct knowledge of surface currents. The strategies to collect or block the spilled oil or to look for a person or a container lost at sea depend on the estimated currents, as they are the main driving mechanism for dispersion.

1.1. The NW Mediterranean Sea

Some environmental properties of the NW Mediterranean are highly conditioned by the fact that it is a virtually enclosed sea. The tides are very small and the circulation is mainly driven by locally generated density gradients and winds. It features local high and low pressure systems controlled by orographic barriers that determine the spatial distribution of winds and land–sea temperature differences. The Pyrenees are a physical barrier that strongly modifies the wind patterns and produces the Mistral and Tramontane winds in France. Their influence can be noticed hundreds of kilometres offshore, carrying cold and dry air over the Mediterranean Sea. These winds are one of the main contributing factors to Mediterranean storms (Flamant et al., 2003). For European countries the most relevant storms are the so-called regional storms, i.e. winter storms. These regional storms are also the highest cause of economic losses in Europe (Munich-Reinsurance-Company, 2004). These extra tropical cyclones generally have less destructive power than tropical cyclones or tornadoes, but they are able to produce damaging winds over a wide area as well as wave damage in

* Corresponding author. Tel.: +44 (0)1517954958; fax: +44 (0)1517954801.
E-mail addresses: rbol@pol.ac.uk (R. Bolaños), osunac@cicese.mx (P. Osuna), jaw@pol.ac.uk (J. Wolf), jaak.monbaliu@bwk.kuleuven.be (J. Monbaliu), agustin.arcilla@upc.edu (A. Sanchez-Arcilla).

1463-5003/$ - see front matter © 2010 Elsevier Ltd. All rights reserved.
doi:10.1016/j.ocemod.2010.10.004

coastal areas. Winter storms can have associated effects such as storm surges, floods, high seas/waves and coastal erosion.

Millot (1999) gives a review of the general ocean circulation patterns in the Mediterranean showing the quasi-permanent slope current that flows from north to south along the French and Spanish coast, the eddies occurring in the African coast and the eddy near the Gibraltar Strait. Other studies (Flexas et al., 2002; Rippeth et al., 2002; Rubio et al., 2009) have given a more detailed description of particular patterns and the origin of oscillations at the Catalan coast.

Fig. 1 shows the study area with the contours of bathymetry; the large bathymetric gradients and changes in continental shelf width are important features of the area.

1.2. Ocean modelling in the Mediterranean

Some interesting features of the Mediterranean circulation include the origin of current meandering (Flexas et al., 2002) and the advection of eddies from the Gulf of Lions (Rubio et al., 2005). It is well known that the ocean dynamics exert a strong control over biology. For instance, Rodriguez et al. (2001) showed the role of mesoscale vertical motion in controlling the size of phytoplankton, and Sabates et al. (2004) linked the concentration and dispersion of larval patches to current meandering.

Measurements of currents and hydrodynamic parameters are sparse and limited in time and space. Thus, a numerical model is needed to complement and extrapolate the information (in time and/or space), to understand physical processes (in process-oriented studies) and to predict the future state of the sea. Ocean modelling in the Mediterranean has been the subject of several studies and research projects such as MFSTEP and MOON. The POM model (Blumberg and Mellor, 1987) has been implemented for the NW Mediterranean (Ahumada and Cruzado, 2007), successfully reproducing the major features of the circulation. Pinardi and Masetti (2000) present a description of the Mediterranean properties derived from observations and modelling, demonstrating a reasonable comparison between model and data. The variability of atmospheric forcing can drive changes in current flow structures. The wind stress is shown to be mainly responsible for transport through the Straits (e.g. Gibraltar). Heat flux was also shown to be a very important forcing of the circulation, a fact presented also by Wu et al. (2000). Bargagli et al. (2002) used the POM model for ocean modelling in the Mediterranean, and in particular the Adriatic Sea, for predicting sea elevation and storm surge, showing that better performance is given by the correct representation of the principal barotropic modes and of the pressure forcing on the basin. The energy spectrum of circulation in the Catalan shelf is dominated by oscillations in the diurnal-inertial band (Rippeth et al., 2002) which were reproduced by using a frictionless, two-layer, analytical model that gave the depth penetration and phase reversal of the oscillations. Jorda (2005) implemented the SYMPHONIE model to study the evolution of a topographic Rossby wave over the continental shelf, the wind effects and exchanges between shelf and slope induced by wind and the slope current. There has also been some work dealing with Lagrangian observation and modelling such as Pizzigalli et al. (2007) who studied the dispersion properties of the Mediterranean using the Modular Ocean Model (MOM) used in the Mediterranean Forecasting System project.

Pre-operational 3D current simulations of the NW Mediterranean have been carried out in the framework of the EU MFSTEP project and the Spanish ESEOO project. The model used is the SYMPHONIE model (Marsaleix et al., 1998), a 3D primitive equations model coded in finite differences. The HIPOCAS project (Hindcast of Dynamic Processes of the Ocean and Coastal Areas of Europe) performed a high resolution hindcast of wind, sea-level and wave climatology for the European waters including the Mediterranean. A re-analysis of the NCEP/NCAR atmospheric model, the WAM wave model and the HAMSOM and TELEMAC models for sea level modelling were used. This data have been very valuable because

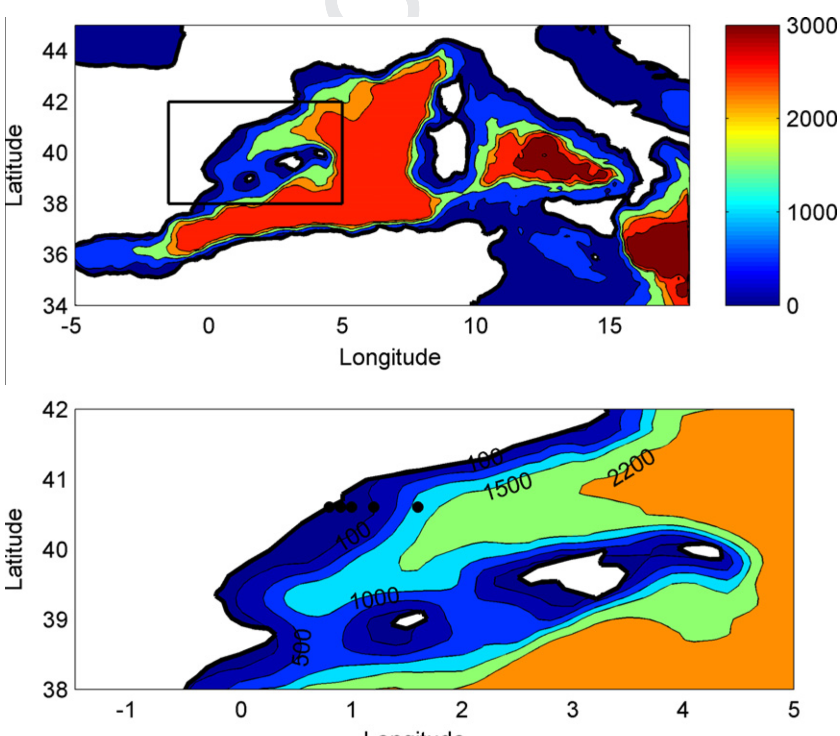

Fig. 1. The upper panel shows the NW Mediterranean including bathymetric contours. The bottom panel shows the Catalan coast and five points (20, 59, 81, 104 and 193 m depth) that have been used to evaluate the model.

they provided a tool for studying long term patterns with high accuracy (Ratsimandresy et al., 2008).

1.3. Wave modelling in the Mediterranean

Regarding wave modelling in the Mediterranean there have been different studies about the wave climate and behaviour of wave models. Cavaleri and Sclavo (2006) use information about waves in the Mediterranean from models, satellites and buoys to obtain calibrated time series of wave properties. Cavaleri (2005) presented a wave atlas for the Mediterranean, based on the ECMWF model and its calibration, to properly take account of properties of a semi-enclosed area such as the Mediterranean. Cavaleri and Bertotti (2004) studied the accuracy of modelled wind and waves in the Mediterranean using the ECMWF atmospheric model and the WAM wave model, finding a direct correlation of the error with fetch. Larger errors are found at short fetches.

The sources of errors in the operational wave modelling for the Catalan coast (Spanish Mediterranean) have been discussed in Bolaños et al. (2004). Errors in prediction of low frequency swell at the buoys appear to be due to errors in the wind fields. The spatial resolution is a very important source of error that affects both wind and wave models. The spatial resolution used to model local wind–wave effects should be suitable to simulate the required details of coastal processes. At the buoy locations there were some local features that have considerable impact on wind patterns and hence on waves. The spatial scale of these phenomena is of the order of a few kilometres and thus a detailed nesting should be implemented in order to be able to simulate the fetch limited wind waves.

Bolaños et al. (2007) used both WAM and SWAN (version 40.11) in the NW Mediterranean to evaluate two wind models (MASS and ARPEGE) when predicting severe storm waves. The SWAN runs show a better agreement in predicting the growing and waning of the storm peaks and seem to reproduce the maximum wave height better. However, both models presented similar accuracy when predicting integrated parameters such as significant wave height, although an analysis of the predicted spectral shape revealed that there are still some more complex processes unaccounted for. SWAN provided a generally larger underestimation of the energy in the low frequency band and a larger overestimation of energy at high frequencies. This cancels out the estimation of total energy (and thus Hs) but produces an underestimation of mean period (note this has been corrected in later versions of SWAN by a modification of the whitecapping and wind input source function (van der Westhuysen et al., 2007)). It was apparent that, in general, WAM predicts the spectral shape better than SWAN. Differences between models are most likely due to the wind input term in which the WAM formulation (Janssen, 1991) enhances growth of younger wind seas while SWAN, using the default (Komen et al., 1984) formulation, is based only on a wind speed and wind dependent drag coefficient.

Several operational products exist which deal with ocean and wave modelling in the Mediterranean such as the Mediterranean Ocean Forecasting System, Poseidon Ocean forecast, MERCATOR, ESEOO, PREVIMER among others. However, those systems treat ocean and wave modelling independently without taking into account any of the possible interactions between waves and currents. For the Catalan coast there has been some pilot research to study wave–current interaction in the context of an operational system (Jorda et al., 2007) showing the importance of the waves on the currents in a microtidal environment. The relative impact of different coupling terms was shown. The wave-modified wind drag coefficient is dominant, although the Stokes drift can also substantially change the circulation forecast. The wave modified bottom drag coefficient is not very important except near the coast (where bottom depth < 10 m).

1.4. Wave–current interaction

Coastal environmental processes do not take place in isolation but interact with each other to form a complex system. There have been a number of research studies dealing with such interactions e.g. atmosphere–waves (Janssen, 1989; Makin and Kudryavtsev, 1999, 2002), wave–current (Mellor, 2003, 2005; Mellor and Blumberg, 2004; Ardhuin et al., 2008), wave–current interactions for rip currents (Yu and Slinn, 2003) and wave–turbulence (Rascle et al., 2006; Rascle and Ardhuin, 2009).

Theoretical work on wave current interaction has been taking place over several decades. Andrews and McIntyre (1978a) derived an exact theory for the interaction of waves with a Lagrangian-mean flow including the wave momentum into the mean flow evolution. Mellor (2003, 2005) derived, with an Eulerian averaging, a set of equations to be used in ocean models based on linear wave theory, assuming a flat bottom. More recently Ardhuin et al. (2008), following the Andrews and Mcintyre work (Andrews and McIntyre, 1978a,b), derived explicit wave-averaged primitive equations limited to 2nd order wave theory. McWilliams et al. (2004) perform a derivation of a set of equations for use in finite water depth. Mellor (2008) presents some corrections for the radiation stress of his previous work.

The main effects of waves on the mean flow commonly considered are due to the radiation stress and Stokes drift, although interaction with turbulence can also be an important process (Babanin et al., 2009). Several numerical, experimental and observational investigations have been done to understand the latter process showing its importance to control the upper ocean dynamics (eg. Polton et al., 2005). Ardhuin et al. (2009) used radar measurements to estimate the Stokes drift current showing that typically it is between 0.6% and 1.3% of the wind speed (the direct wind induced current is about 1–1.8% the wind speed). Lane et al. (2007) performed a study of radiation stress and the vortex force showing that both comprised all the conservative effects of waves on currents, the vortex force being larger.

Rascle et al. (2006) studied the Stokes drift and mixing with a one-dimension model showing that the surface drift reaches 1.5% of the wind speed. Weber et al. (2006) showed that the Eulerian and Lagrangian approaches for the fluid motion produce the same mean wave induced flux in the surface layer: for their simulations the wave induced stress constituted about 50% of the total atmospheric stress for moderate to strong winds.

A coupled 2D current-wave model using an unstructured grid applied to a hurricane in the Gulf of Mexico and a storm in the Adriatic Sea (Roland et al., 2009) shows the importance of considering wave effects when modelling water levels. The wave effect was a surface stress due to radiation stress. Tang et al. (2007) implemented a wave–current interaction formulation in a 3D ocean model (POM) and a spectral wave model (WAVEWATCHIII) following Jenkins (1987) formulation and evaluated the model by comparison with surface drifters. They showed that the Stokes drift was the main dominant effect with a contribution of about 35%. They also show a reduction of momentum transfer from wind to currents if waves are taken into account.

Feddersen (2004) studied the effect of directional spreading on the radiation stress showing it was the main reason for the differences between measured and estimated (narrow band) radiation stress. Wave–current interaction has also been studied in a flume observing unexpected changes in the mean horizontal wave profile (Groeneweg and Battjes, 2003) and wave induced mixing (Babanin, 2006).

Qiao et al. (2004) used a parameter to estimate wave induced mixing and applied it to ocean forecasting showing improved agreement with data. In a similar way Babanin (2006), assuming a wave Reynolds stress, showed the upper ocean mixing under waves; such parameterisation was confirmed under laboratory flume and good mixed layer depth estimations were obtained.

The main objectives of the present work are first to perform a good qualitative ocean modelling of the NW Mediterranean with POLCOMS, secondly to implement novel three-dimensional wave–current interaction terms in an ocean model (POLCOMS) and a third generation spectral wave model (WAM) which improves the physics considered in the system; and finally to evaluate the sensitivity of the different forcing terms such as atmospheric forcing and initial conditions. The evaluation of the sensitivity to wave–current interaction will be limited to Stokes drift only. Radiation stress effects are expected to be too limited for the spatial resolution of the current implementation. Note that POLCOMS has been implemented for different areas such as the Irish Sea (Osuna and Wolf, 2005) and the North Sea (Holt and James, 1999), but not for the Mediterranean Sea. WAM has been validated for the Mediterranean by for example Cavaleri and Bertotti (2004) and Bolaños et al. (2007) and has been used extensively worldwide for wave forecasting and hindcasting.

2. The POLCOMS–WAM model

2.1. POLCOMS

The POLCOMS (Proudman Oceanographic Laboratory Coastal-Ocean Modelling System) is a three dimensional primitive equation numerical model formulated in a spherical polar, terrain following coordinate system (sigma coordinates) and on a B-Grid (Holt and James, 2001). It solves the incompressible, hydrostatic, Boussinesq equation of motion separated into depth varying and depth independent parts to allow time splitting between barotropic ($\bar{u}$) and baroclinic (u_r) components. The eastward velocity is then $u = \bar{u} + u_r$ and the northward component is $v = \bar{v} + v_r$ The turbulence closure scheme uses Mellor and Yamada (1974, 1982) with a modification proposed by Craig and Banner (1994) to take into account surface wave breaking. The system has been structured to allow its execution on parallel and serial computers (Ashworth et al., 2004). The depth varying components are (Holt and James, 2001; Proctor and James, 1996):

$$\begin{aligned}\frac{\partial u_r}{\partial t} &= -L(u) + f v_r + \frac{uv\tan\phi}{R} - \prod_{\gamma} + D(u) - H^{-1}[F_S - F_B] - NLB_{\chi}\\ \frac{\partial v_r}{\partial t} &= -L(v) + f u_r + \frac{u^2\tan\phi}{R} - \prod_{\phi} + D(v) - H^{-1}[G_S - G_B] - NLB_{\phi}\end{aligned} \tag{1}$$

where $L(u)$ is the advection terms; $f v_r$, the Coriolis acceleration; $\frac{uv\tan\phi}{R}$, the correction for projection; $\prod_{\lambda}$, the buoyancy terms; $D(u)$, the diffusion term (replacing the vertical stresses), with Kz eddy viscosity; $H^{-1}[F_S - F_B]$, the terms related to surface and bottom stresses; NLB_{χ}, the depth means of the nonlinear and buoyancy terms; R, the radius of the earth.

The depth mean equations are:

$$\begin{aligned}\frac{\partial \bar{u}}{\partial t} &= f\bar{v} - (R\cos\phi)^{-1}\left[g\frac{\partial\zeta}{\partial_{\chi}} + \rho_0^{-1}\frac{\partial P_a}{\partial_{\chi}}\right] + H^{-1}[F_S - F_B] + NLB_{\chi}\\ \frac{\partial \bar{v}}{\partial t} &= f\bar{u} - (R)^{-1}\left[g\frac{\partial\zeta}{\partial_{\phi}} + \rho_0^{-1}\frac{\partial P_a}{\partial_{\phi}}\right] + H^{-1}[G_S - G_B] + NLB_{\phi}\end{aligned} \tag{2}$$

where $f\bar{v}$ is the Coriolis term; $(R\cos\phi)^{-1}\left[g\frac{\partial\zeta}{\partial_{\chi}} + \rho_0^{-1}\frac{\partial P_a}{\partial_{\chi}}\right]$, the buoyancy terms; $H^{-1}[F_S - F_B]$, $H^{-1}[G_S - G_B]$, the terms related to surface and bottom stresses; NLB_{χ}, depth means of the nonlinear and buoyancy terms.

The model also includes explicitly a horizontal diffusion term which alters the velocity, temperature and salinity fields. The parameters fields are interpolated onto z-levels and multiplied by a depth-dependent diffusion coefficient (Wakelin et al., 2009).

POLCOMS has been used on the Northwest European continental shelf to model the hydrodynamics, ecosystem and tidal mixing (Siddorn et al., 2007; Holt and Umlauf, 2008), estuary dynamics (Moore et al., 2009) and real time forecasting system in the Irish Sea (Krivtsov et al., 2008). For a detailed description of POLCOMS the reader is referred to Holt and James (2001) and Proctor and James (1996).

2.2. WAM

The WAM is a third generation wind–wave model developed during the 1980s. It solves the energy balance equation (WAMDI-Group, 1988; Komen, 1994). The model simulates the 2D wave spectral evolution, considering the energy input by wind, energy dissipation by whitecapping, non-linear wave–wave interactions and bottom friction. The action balance equation can be expressed as:

$$\frac{\partial F}{\partial t} + \frac{\partial}{\partial x}(c_x F) + \frac{\partial}{\partial y}(c_y F) + \frac{\partial}{\partial \theta}(c_{\theta F}) + \sigma\frac{\partial}{\partial\sigma}\left(c_{\sigma}\frac{F}{\partial}\right) = S \tag{3}$$

where $F(\sigma, \theta, x, y, t)$ represents the spectral density; σ is the frequency; θ, the wave direction; y and x latitude and longitude, respectively, t is time. The c_x, c_y, $c_{\theta,}$ $c\sigma$ terms represent the wave propagation speed in the different parameter spaces. The right-hand side represents all effects of generation and dissipation of the waves including wind input S_{in}, whitecapping dissipation S_{ds}, non-linear quadruplet wave–wave interactions S_{nl} and bottom friction dissipation S_{bf}. A detailed description of the WAM model can be found in WAMDI-Group (1988) and Komen et al. (1994). One can show that Eq. (3) is equivalent to the action density conservation equation. This is important in the presence of currents since wave action and not wave energy is conserved (Ozer et al., 2000). Monbaliu et al. (2000) modified WAM to take into account high resolution scales more suitable for shallow water regions.

2.3. POLCOMS–WAM coupling

The POLCOMS and WAM models have been coupled in a two dimensional (depth-averaged), two way mode to consider several processes taking into account the wave refraction by currents, bottom friction by currents and waves and enhanced wind drag due to waves (Osuna and Wolf, 2005). The wave current interaction module was developed to allow the synchronous exchange of information between POLCOMS and WAM: WAM is embedded in the baroclinic step of the hydrodynamic model. Data passed from POLCOMS to WAM include barotropic and bottom layer current components and water depth updated every baroclinic time step. Time-interpolated wind components are also transferred from POLCOMS to WAM within a moving framework according to the barotropic current components (Osuna and Wolf, 2005). Data passed from WAM to POLCOMS are used to modify the surface wind stress. In POLCOMS a wind dependent drag coefficient (Smith and Banke, 1975) is used, namely, $C_D = (0.63 + 0.066U_{10}) \times 10^{-3}$ when the coupled system is used the wind stress is estimated considering the wave field following Janssen (1991). The effect of the coupling at the bottom due to the presence of waves and currents is estimated using the Madsen (1994) formulation.

Osuna and Wolf (2005) presented an evaluation of wave–current coupling using POLCOMS–WAM system in the Irish Sea, and showed differences of up to 15% in Hs associated with waves and currents travelling in opposite directions. Changes in mean period (Tm02) due to Doppler shifting reached 20%. Differences in apparent bottom roughness were of one order of magnitude. The effect of waves on the currents was less evident. Validation with data at a point in 23 m depth showed little effects (5% for wave parameters, 2.5% sea surface elevation, 10 cm/s for current velocity (10%). The model has also been used for storm surge modelling (Brown and Wolf, 2009) showing an improvement of the prediction when considering wave surface roughness by implementing the Charnock formulation and using Janssen (1991).

In order to progress the POLCOMS–WAM coupling development, in the framework of the EU MARIE project (http://lim050.upc.es/projects/marie), three dimensional interaction processes such as Stokes drift, radiation stress and Doppler velocity, which allow vertical current shear to be included, have been implemented following the approach described by Mellor (2003, 2005). However, the radiation stress term is not going to be discussed in the present work since, as mentioned above, its effects in the Mediterranean at the scales used in this paper, are expected to be small. The full details of the derivations can be found in the original papers. Individual terms are described below.

2.3.1. Stokes drift

Stokes drift is a well known higher order wave process which describes the mean surface drift due to waves. The behaviour of the Stokes drift has been studied theoretically, measured and modelled in several ways. Rascle et al. (2006) studied the upper ocean dynamics showing an important surface shear due to the Stokes drift, the different Stokes drift estimations for sea and swell waves and the effect of the Stokes drift combined with the Coriolis force on Eulerian velocities over the whole water column, leading to current magnitudes of 20–30% of the wind induced currents. Lewis and Belcher (2004) showed that the effect of the Stokes drift in the Ekman layer gives a better approximation when describing the angular rotation of the current profile. Smith (2006) studied the effect of the Stokes drift from measurements with an Eulerian approach showing that the Stokes drift is intermittent and might be related to the groupiness of waves.

The Stokes drift effects have been considered following the formulation of Mellor (2003, 2005), defining the Stokes velocity for a 2D directional spectrum as:

$$U_{S\propto} = 2g \int_{\theta} \int_{\sigma} \frac{k_{\alpha}}{c} \frac{\cos h2kD(1+\zeta)}{\sin h2DKD} F \,\partial\sigma\,\theta \tag{4}$$

where α refers to the x or y component of the Stokes velocity vector $U_{S\alpha}$ (and of the wave number vector k), c is the respective wave celerity, D water depth, $F(\sigma, \theta)$ the wave energy spectrum, g acceleration due to gravity. θ and σ are the direction and frequency of each spectral component. ς is the sigma coordinate. After the inclusion of the above term, the velocity in Eq. (1) includes the Stokes drift effect such that $u = \bar{u} + u_r + U_{S\propto}$.

2.3.2. Doppler velocity

The Doppler velocity that modifies the wave dispersion relation is evaluated according to the expression based on Kirby and Chen (1989) analysed and described by Mellor (2003), and is defined as:

$$u_{A\alpha} = 2\int_{-1}^{0} u \frac{kD\cos h2kD(1+\zeta)}{\sin h2kD}\,\partial\zeta \tag{5}$$

where u represents the total velocity.

2.3.3. Surface stress partitioning

In order to be consistent in terms of conservation of momentum in a fully coupled system, the distribution of surface stress between waves and currents has to be considered. Thus, the surface stress felt by the mean circulation (τ_c) is the total wind stress (τ_a) minus the stress acting on waves (Janssen et al., 2004):

$$\tau_c = \tau_a - \rho g \int_0^{2\pi} \int_0^{w_h} \frac{k}{w}(S_{in} + S_{nl} + S_{ds})\,dw\,d\theta \tag{6}$$

where τ_a is the wind stress and it is equal to $\rho_a u_*^2$ in which ρ_a is the air density and u^* the wave-modified air friction velocity which is estimated following Janssen (1991).

An interesting effect for the stress felt by the currents is the balance between the total air stress (τ_a) and the net stress going into the waves. This balance depends on the wave age: under developing waves the stress felt by the mean circulation (τ_c) will be reduced, while in decaying waves it would be increased. This panorama might change at shallow/intermediate water depth where bottom friction and wave breaking (even without wind at all) can induce extra momentum and mixing (Gemmrich and Farmer, 2004; Longo et al., 2002).

2.4. Effect of the Coriolis–Stokes term

The effect of the Coriolis–Stokes (CS) term on the Ekman current profile has been described by a number of authors (Hasselman, 1970; Xu and Bowen, 1994; Polton et al., 2005; Rascle et al., 2006; Rascle and Ardhuin, 2009). They conclude that the CS forcing significantly changes the mean current profile, similar to the addition of a surface stress at right angles to the wind.

In order to illustrate the implementation of the CS term, an idealized one point version of the system, located at 43.4°N latitude, has been implemented. In this idealized case, a 300 m depth is used and no effects of stratification are considered. In order to compute the vertical turbulent fluxes, a Mellor-Yamada 2.5 level closure scheme, adapted by Craig and Banner (1994) is used. The model is forced by a constant wind of 10 m/s blowing to the east (surface stress is 0.16 N/m^2, as no effect of waves is considered for this case, according to the value computed using the Smith and Banke (1975) standard formula in POLCOMS). Considering this value for the surface stress, the friction velocity in the water is $u^* = 1.25 \times 10^{-2}$ m/s. After several days, the wave field reaches a stationary state, with a significant wave height of 2.36 m and a peak period of 8.4 s.

In Fig. 2, the vertical profiles of the normalized wind driven current computed by POLCOMS with the CS effect (POLCOMS + CS), that computed by POLCOMS without CS, the effect of the CS term (δ_u and δ_v; i.e. POLCOMS + CS minus POLCOMS), and the Stokes drift (u_s, u_v) components are shown. The profiles are normalized using the friction velocity in the water (u^*). It is observed that the Stokes drift u_s component is comparable to the maximum wind driven u component, but its effect is constrained to an upper fraction of the layer (about 10 m), while the CS effect penetrates deeper in the two wind driven components.

The negative values of the CS term effect (δ_u and δ_v), indicate a further rotation of the current components to the right of the standard Ekman circulation (in northern hemisphere), as can be seen in Fig. 3. As pointed out by Polton et al. (2005) and Rascle et al. (2006), this spiral shift is in qualitative agreement with the differences observed between measurements and classical Ekman circulation.

3. Model setup for the Mediterranean

3.1. Model grids

The POLCOMS–WAM was implemented for the NW Mediterranean Sea with a spatial resolution of 0.1° [O(10 km)] extending

Please cite this article in press as: Bolaños, R., et al. Development of the POLCOMS–WAM current–wave model. Ocean Modell. (2010), doi:10.1016/j.ocemod.2010.10.004

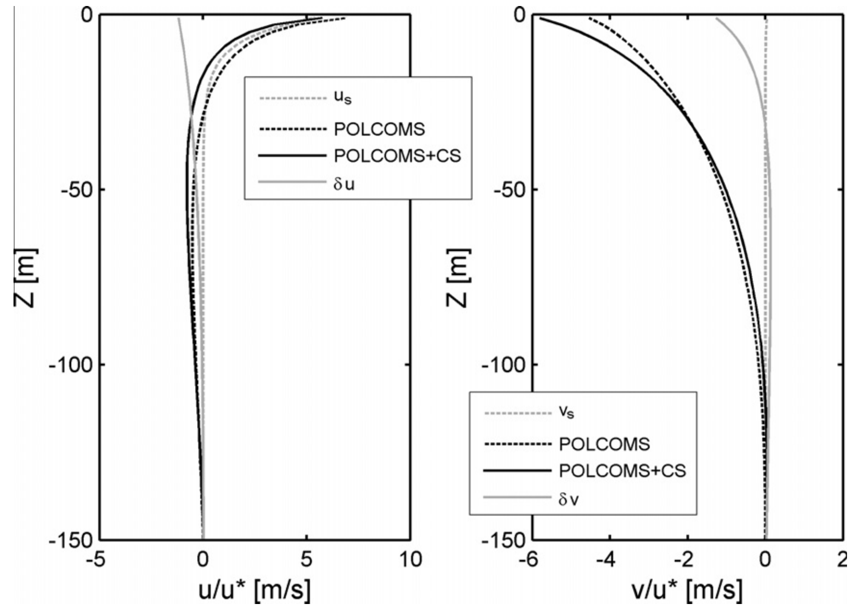

Fig. 2. Current components computed with and without considering the Coriolis–Stokes effect and the contribution of the CS term, as well as the Stokes components. The values are normalized by the friction velocity.

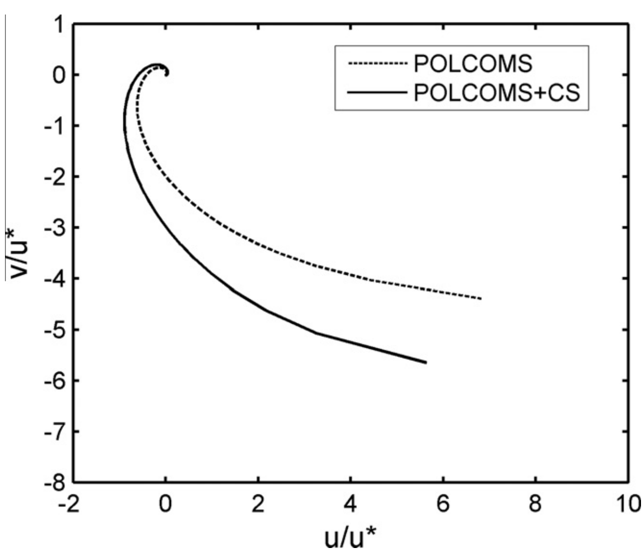

Fig. 3. Hodograph of current velocities computed by POLCOMS and POLCOMS + CS. The values are normalized by the friction velocity.

from −5° W to 18° W longitude and 34° N to 45° N latitude (Fig 1) with 20 sigma levels. For the vertical distribution, due to the large depths found in the Mediterranean, a modification of the sigma coordinates (S Coordinates) was used which allows more vertical levels at the surface. The distribution of the S coordinates is defined as (Holt and James, 2001):

$$\sigma_{k-0.5} = S_k + \frac{h_{i,j} - h_c}{h_{i,j}}[C(S_k) - S_k] \quad h_{i,j} > h_c \tag{7}$$

$$= S_k \quad h_{i,j} \geqslant h_c$$

$$S_k \quad N-1 \text{ evenly spaced levels}$$

$$C(S_k) = (1-B)\frac{\sinh(\theta S_k)}{\sinh(\theta)} + B\frac{\tanh[\theta(S_k + 0.5)] - \tanh(0.5\theta)}{2\tanh(0.5\theta)}$$

$$h_c = 100, \quad \theta = 5, \quad B = 0.25$$

where θ and B are parameters that increase resolution at the surface for depths larger than h_c.

For the open boundary conditions (strait of Gibraltar and southeast corner of the domain) the model used a radiation boundary condition without any temperature, salinity or current forcing. The system was run for 30 days (720 h) with the initial conditions from climatology (see below) and wind velocity set to zero, then the model was forced with the storm of November 2001 (about 12 days duration). Air temperature, cloud cover, humidity and atmospheric pressure were considered as constant for this time. WAM was run on the same spatial grid with a resolution of 25 frequencies and 24 directions and the physics of cycle-4 (Komen, 1994).

3.2. Initial conditions

Initial conditions were taken from climatological data (http://www.bo.ingv.it/mfstep/WP8/clim_data.htm) which consist of 3D fields of temperature and salinity with a 0.25° resolution and 35 vertical levels based on the MEDATLAS data bank using the MODB (Mediterranean Oceanic Data Base analysis technique (Brasseur et al., 1996)). Therefore horizontal and vertical interpolations were needed. The resulting fields were smoothed by a local averaging. Temperature and salinity profiles are shown for a point off the Catalan coast in 104 m depth (Fig. 4). A surface temperature of about 17 °C in a well mixed layer of about 20 m depth can be seen, the temperature then decreases down to 14 °C at about 60 m depth; below that depth temperature is relatively constant. Salinity increases from the 20 m depth down to the bottom reaching values of 38.4 ppt. For the NW Mediterranean, being a microtidal environment, the water density distribution is expected to play a very important role in driving the ocean dynamics.

3.3. Atmospheric forcing

The atmospheric forcing consisted of two main periods. One was of 720 h with the objective of spinning up the model with wind velocity set to zero and constant air temperature (15°), air pressure (1000 mb), humidity (50%) and cloud cover (50%). After this period the model was forced with winds from the MASS model (Mesoscale Atmospheric Simulation System) (Codina et al., 1997; MESO, 1994) for November 2001 when a severe wind and wave

Please cite this article in press as: Bolaños, R., et al. Development of the POLCOMS–WAM current–wave model. Ocean Modell. (2010), doi:10.1016/j.ocemod.2010.10.004

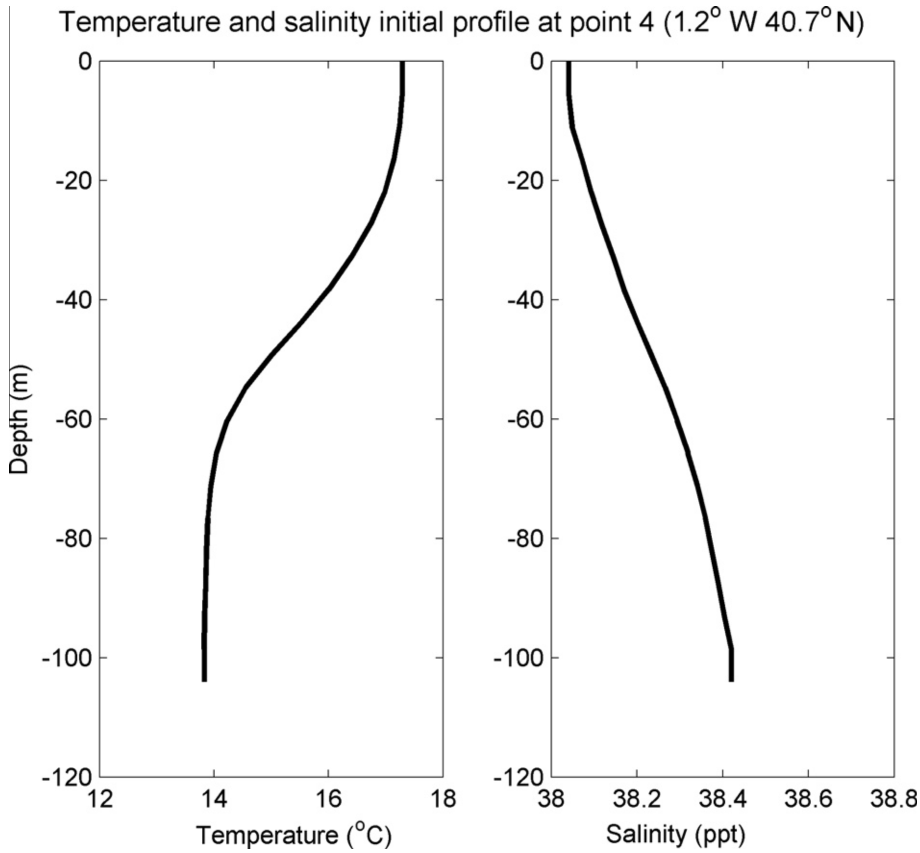

Fig. 4. Temperature (left) and salinity (right) initial condition profile at a location (1.2°W 40.7°N) in the Catalan coast with 104 m depth (see Fig. 1).

storm occurred. Air temperature, pressure, humidity and cloud cover were set to the same constant values as the spin up period.

The wind and waves for the November 2001 storm have been described and validated versus QuikSCAT and coastal meteorological stations by Bolaños et al. (2007): on November 10th a low pressure system occurred over the NW Mediterranean while a high pressure centre was located in the NE Atlantic. On November 11th pressure gradients increased, producing the first storm peak. Subsequently, the system relaxed until the 15th when another low pressure system was generated over the NW Mediterranean producing a second storm peak recorded by the buoys. Strong winds of up to 18 m/s were measured at the Ebro delta. Significant wave height reached about 8 m in the NW Mediterranean and 6 m at the Catalan coast. The spatial resolution of the modelled winds was 0.16°. Fig. 5 shows the time evolution of the spatial mean wind for the full period. It can be seen that this was a severe storm with average wind over the whole NW Mediterranean of more than 10 m/s during the storm peak.

From an operational and validation point of view these settings may produce errors due to the crude representation of initial conditions and the atmospheric forcing, but for the assessment of the terms for general conditions the settings proved to be sufficient. The model was run several times in order to evaluate different processes. Table 1 shows the description of each run and the processes included. All the model runs included temperature and salinity initial conditions, the reference run (POLC-ref) is only forced by these initial conditions and thus it includes only the thermohaline circulation. The POLC-ATM run included the atmospheric forcing, estimating the wind stress using Smith and Banke (1975). The POLC-WAM2D included the atmospheric forcing and the modification of the wind stress by waves as Janssen (1991) (see Section 2.3). The POLC-WAM3Dstok includes atmospheric forcing, wave-modified wind stress and the Stokes drift (se Eq. (4)) and POLC-WAM-

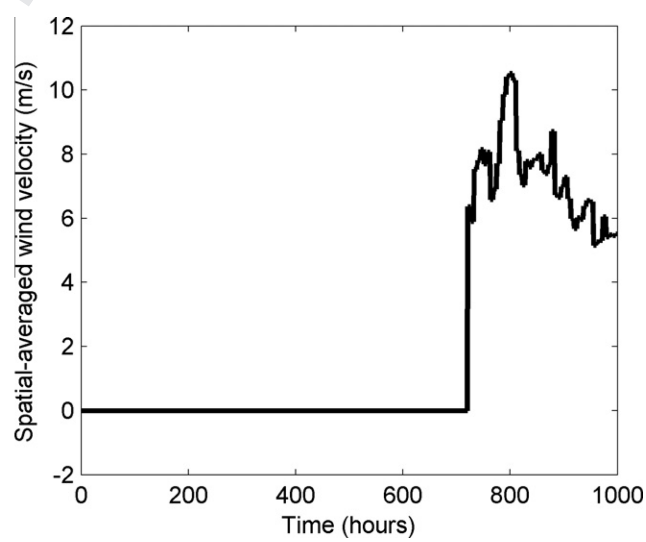

Fig. 5. Time evolution of the mean spatial wind velocity. First 720 h is the spin up period.

stress run was with atmospheric forcing, wave-modified wind stress and the partitioning of surface stress between currents and waves (see Eq. (6)).

4. Results

4.1. Reference run – thermohaline circulation

Fig. 6 shows the surface velocity in the NW Mediterranean after the spin up period, with thermohaline forcing only, showing that

Table 1
Runs of the model and processes included.

Run	T and S initial conditions	Atmospheric forcing	Wave-modified wind stress	Stokes drift	Wave stresses
POLC-ref	X				
POLC-ATM	X	X			
POLC-WAM2D	X	X	X		
POLC-WAM3Dstok	X	X	X	X	
POLC-WAMstress	X	X	X		X

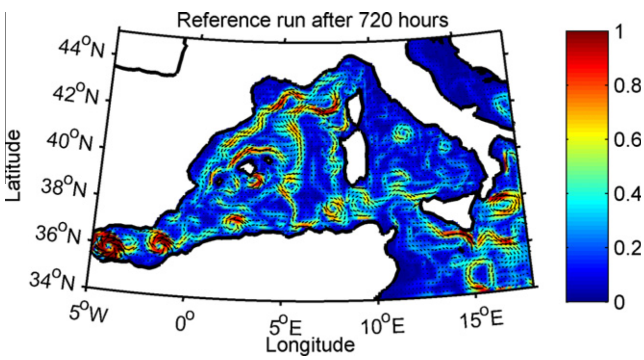

Fig. 6. Surface current distribution after the spin up period (units are m/s).

the model reproduces some features of the Mediterranean surface currents properly, at least from a qualitative point of view. The spatial mean surface velocity is of about 0.29 m/s. The model is able to reproduce the well known Northern current, the eddies near the Gibraltar Strait, the clockwise eddies at the African coast and the current north of Ibiza and Mallorca. These features have been described by Millot (1999). Modelled velocities are larger than expected, which might be due to the lack of horizontal diffusion and/or the coarse representation of bathymetry due to the spatial resolution used. Open boundaries seem to produce some local artificial effects generating large velocities. The run shows that the main hydrodynamic properties of the NW Mediterranean are driven by the density distribution. This run was then used as a reference to evaluate the relative importance of different processes.

4.2. Effect of forcing terms on surface currents

Fig. 7 shows the effect of different processes on the surface currents (mean difference of the surface current field). The main effects are due to the atmospheric forcing and modified wind stress, both presenting similar patterns. To second order there is the Stokes drift with an effect of about 1–5% of the thermohaline circulation. The effect of considering partitioning of stress is a reduction of velocity because part of the wind stress goes into waves. The wave-modified stress changes the wind-driven part of the current, and therefore, this could be important in areas where currents are partially controlled by wind. This might change in coastal areas where wind may play a smaller role (Broche and Forget, 1992). As shown by the reference run, the dynamics are highly controlled by the salinity and temperature distribution, wind and wave effects present effects of the order of 5–20% the thermohaline circulation.

4.3. Effects on surface temperature and salinity

The effect of the forcing terms on salinity and temperature is shown in Fig. 8. For temperature, the main effect is due to atmospheric forcing which refers to wind induced mixing and also to the heat transfer between atmosphere and ocean. During the spin up period a rise in temperature can be produced by the atmospheric forcing due to heat transfer, once the storm starts there is a reduction due to an increased mixing of the water column. The main wave effect is due to the modified wind stress. Stokes drift gives only very minor changes in the mean surface temperature. The changes in salinity are small, the main effect is due to atmospheric forcing, then wave-modified wind stress. Stokes drift effects are one order of magnitude smaller. The consideration of the stress partitioning produces a rise in temperature and reduction of salinity due to a reduced stress into currents (and thus less wind induced mixing).

Fig. 9 shows a detail at the Catalan coast of the storm-average spatial distribution of salinity (right column) and temperature (left column). Differences between salinity distributions are less evident than for the surface current and temperature cases. The main process affecting the surface temperature is the atmospheric forcing; the lack of wind forcing (POLC-ref) produces a higher temperature of the Catalan Sea than the cases with atmospheric forcing

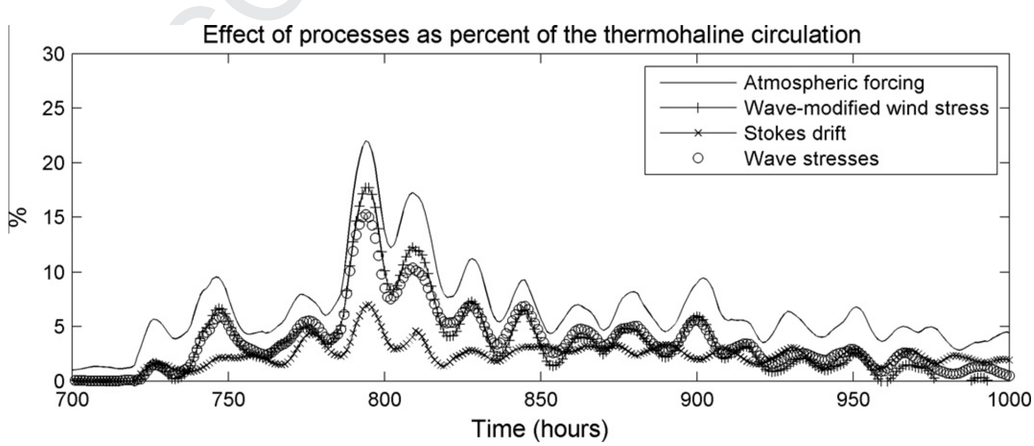

Fig. 7. Effect of processes on spatial-mean surface current represented as percent of the thermohaline circulation.

Please cite this article in press as: Bolaños, R., et al. Development of the POLCOMS–WAM current–wave model. Ocean Modell. (2010), doi:10.1016/j.ocemod.2010.10.004

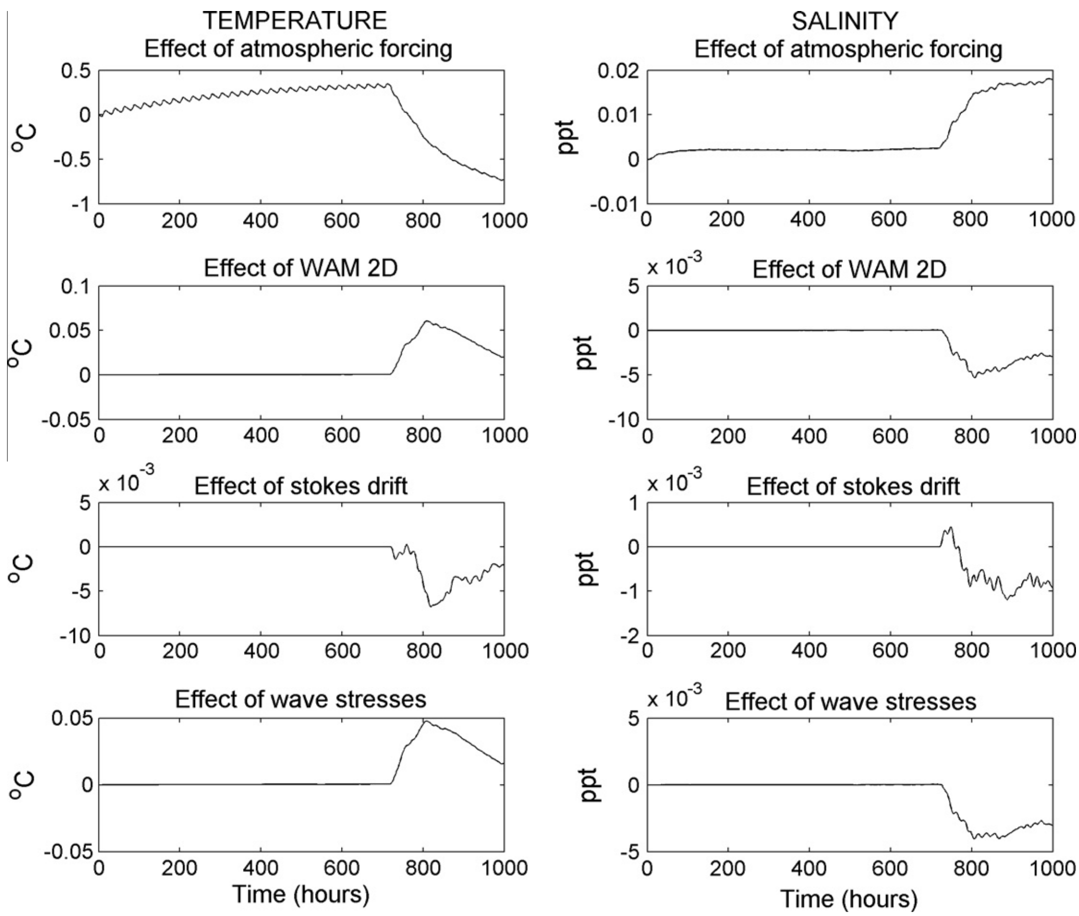

Fig. 8. Effect of terms (atmospheric forcing, wave-modified stress, Stokes drift and surface stress partitioning) on mean surface temperature (left column) and mean surface salinity (right column).

(eg. POLC-ATM). Stokes drift effects are small and the main wave effect is due to modified wind stress.

4.4. Effects on pointwise temperature, salinity and velocity profiles

For the shallow water location (O(20 m), Fig. 10), the profiles are very similar for most of the runs, differences are evident for the run without atmospheric forcing in which the profile evolves to a stratified water column. The effect of the atmospheric forcing is very evident during the storm period in which the water column becomes well mixed. Wave effects are small, up to 0.5° (during a short period of time). Mixing is mainly wind induced and an additional mixing term from waves such as suggested by Qiao et al. (2004) would not be necessary, at least for these atmospheric conditions, as the water column in the nearshore area is mixed. Profiles of salinity show similar behaviour; atmospheric forcing is the largest forcing in the distribution of salinity in the water column. The effect of waves shows little difference in the profiles which suggest that the mixing of the water column occurs mainly due to the direct wind effect.

For a depth of 60 m (not shown) the full water column requires more time to mix. The atmospheric forcing is able to mix the full water column and the time rate of this effect is about 0.3 m/h. At 80 m (Fig. 11) the mixing started to be limited at the bottom, wind is the main forcing mixing the surface water column during the storm event. The atmosphere heat transfer has also an impact changing the temperature of the surface layer (see POLC-ref during 400–700 h). Wave effects are second order, temperature and salinity distributions with Stokes drift and wave-modified wind stress remain similar to the run without wave effects. The rate of deepening of the thermocline (a measure of mixing) is slower compared to the shallower location.

The velocity profiles for the location at 80 m depth are shown in Fig. 12. The total effect of waves is to reduce the velocity in the profile compared to the case of atmospheric forcing, this is due to the consideration of surface stress partitioning. The atmospheric forcing during the spin up period (wind set to zero) does not change considerably the pattern from the reference run, thus atmospheric effects on currents are mainly due to wind and not due to changes in the temperature due to heat transfer. Wind is able to produce a localized rise in surface current during the peak of storm that penetrates up to about 40 m depth, changes observed in deeper parts are related to wind induced changes in the mesoscale circulation taking place in the nearby area.

4.5. Effects on waves

Due to the low currents near the coast, the effect on waves at the coastal points are barely perceptible showing maximum differences of about 0.1 m (2.5%) in Hs. Differences in Tz are also hardly noticeable being up to 0.3 s near the coast. Fig. 13 shows the mean spatial distribution of Hs and mean period during the storm event. The effect of the northern current is evident as well as the effect of some large velocities near the east open boundary and the eddy close to the Gibraltar Strait. Due to the Doppler shift the currents produce a slight increase in mean period with changes of up to 1 s. This effect could be overestimated due to the large currents produced by the reference run (eg. Northern current magni-

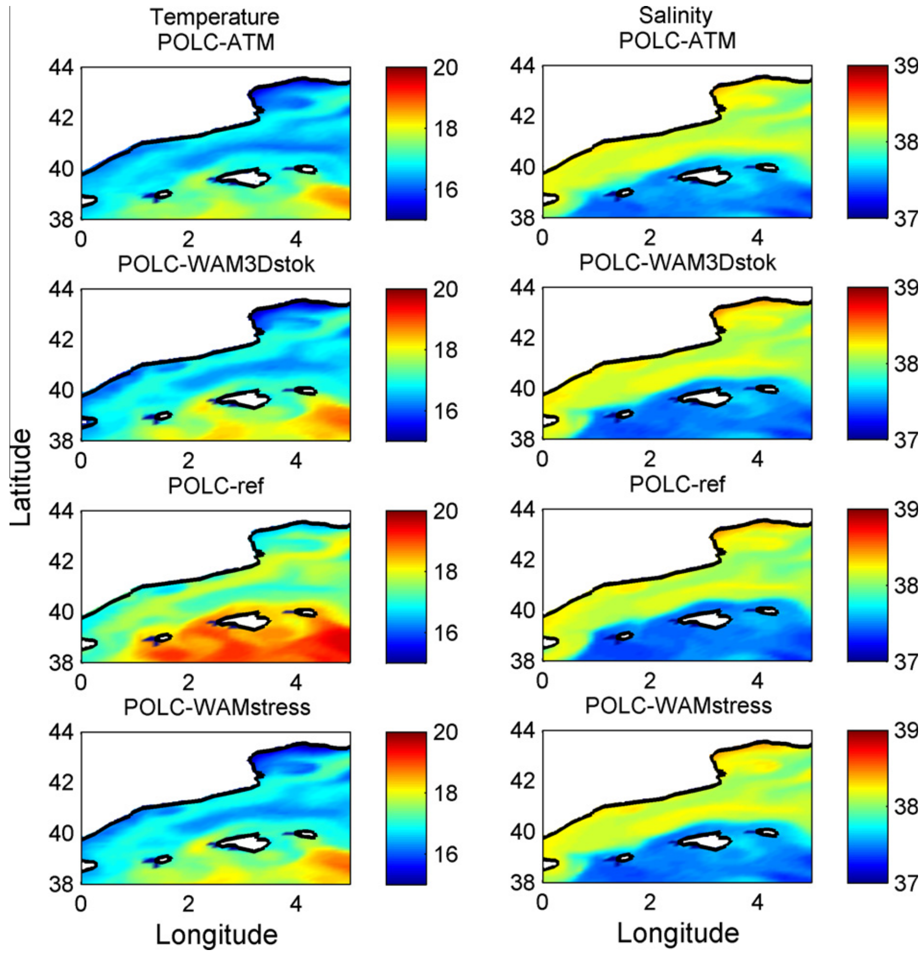

Fig. 9. Time averaged distribution of surface temperature and surface salinity for different model runs.

tude > 0.5 m/s while observations are in the order of 0.3–0.5 m/s (Conan and Millot, 1995)), thus the effect on waves are expected to be even smaller.

5. Discussion

5.1. POLCOMS for the Mediterranean

The POLCOMS ocean model has proved to be able to simulate the main NW Mediterranean properties despite the assumptions required to run it. The spatial resolution is not detailed enough to resolve the Rossby radius of deformation in the Mediterranean and it does not properly resolve the large bathymetric gradients. The initial conditions from climatological data interpolated in the vertical and horizontal showed realistic behaviour and a spin up period of only 1 month was necessary to reach a stable and "realistic" situation. These results show that POLCOMS can be used for proper ocean modelling in the NW Mediterranean and that these settings are good enough to perform an evaluation of the different forcing terms. Further effort has to be done if a full validation of the model is needed, such as increasing spatial resolution, and probably extending the domain to the whole Mediterranean in order to avoid open boundary problems. The northern current appears to be very persistent; the proper prediction of this might be influenced by the spatial resolution in order to resolve the continental slope accurately. The reference run showed that temperature and salinity are very important parameters as they are the main drivers producing the most important features of the Mediterranean circulation. Wind is not the main forcing of current patterns, as was also pointed out by Font (1990) who showed that at the Catalan coast the wind is not responsible for the main characteristics of the marine circulation and indicated that mesoscale activity is probably associated with variations of the density structure.

5.2. Effect of atmospheric forcing

The atmospheric forcing is the main external agent for the general distribution of variables (velocity, temperature and salinity) in the horizontal and vertical and can drive changes in current flow. Wind induced mixing was evident in the storm period, being able to reach a depth of more than 80 m. The surface current velocity is affected by wind which modifies the background density currents. The heat transfer between the ocean and atmosphere also plays a very important role in these simulations. The use of constant air temperature and cloud cover modifies the distribution of surface water temperature by about 0.5° (e.g. Fig. 8, top-left panel). Thermohaline circulation is thus caused by the joint effect of thermohaline forcing and turbulent mixing and it requires surface input. The density distribution determines circulation and is itself affected by currents and mixing of any kind. There are thus two distinct forcing mechanisms that will interact, changes in the wind stress will produce changes in thermohaline circulation; and changes in density distribution (stratification) will modify wind driven currents. Wind induced currents were in the order of 10–20% the thermohaline circulation.

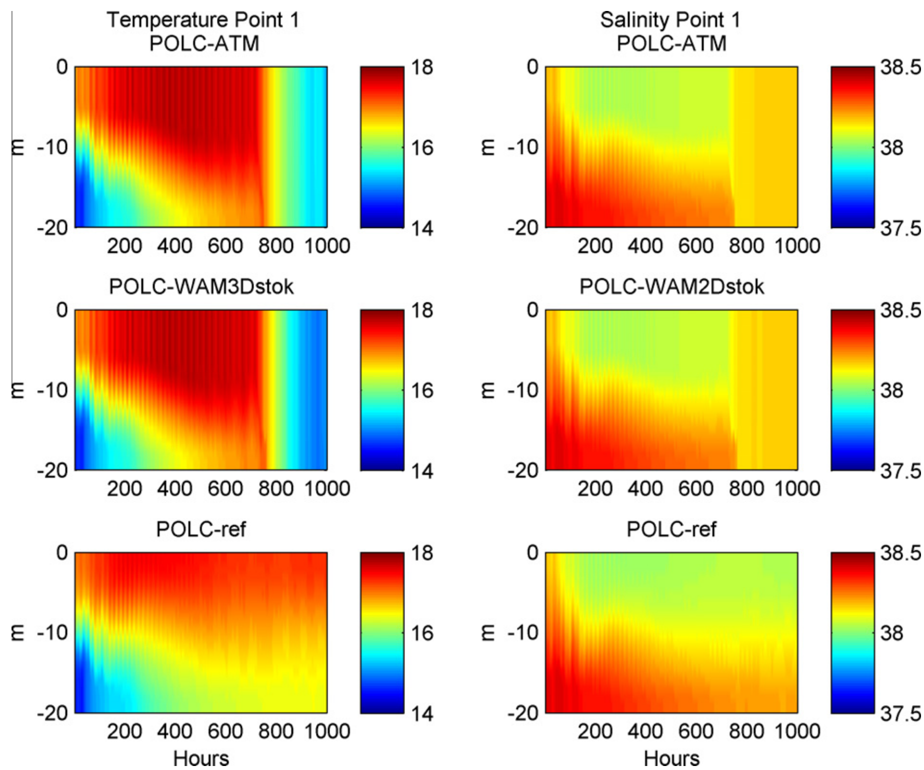

Fig. 10. Profile evolution of temperature and salinity for different runs at a location with 20 m depth (0.9°W 40.7°N).

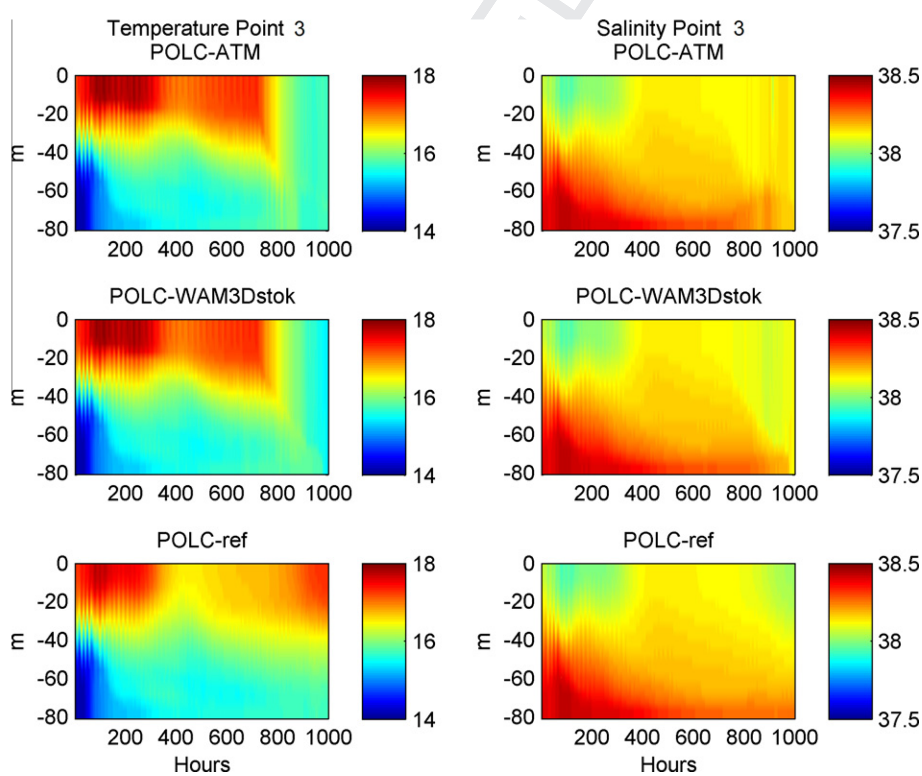

Fig. 11. Profile evolution of temperature and salinity for different runs at a location with 83 m depth (1.1°W 40.7°N).

760 *5.3. Open boundary effects*

761 It is well known that open boundaries are a cause of inconsistencies in ocean models and therefore many people have paid attention to this (Blayo and Debreu, 2005; Lavelle et al., 2008). A proper study of the effect of the boundary conditions for the present application requires more tests with different boundary properties but this is beyond the scope of the present work. For

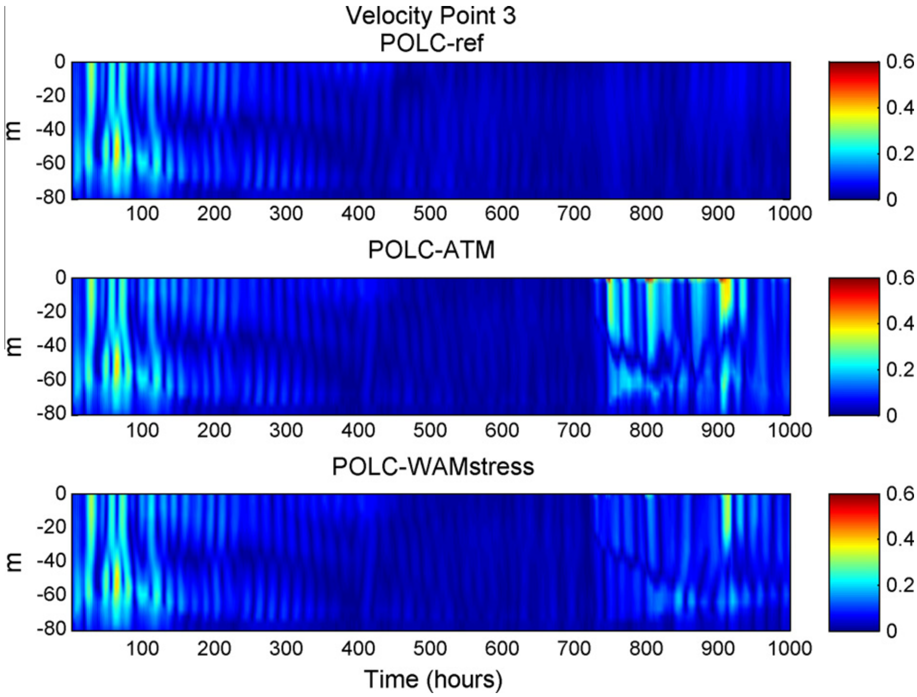

Fig. 12. Velocity profile evolution at (1.1°W 40.7°N) for different runs.

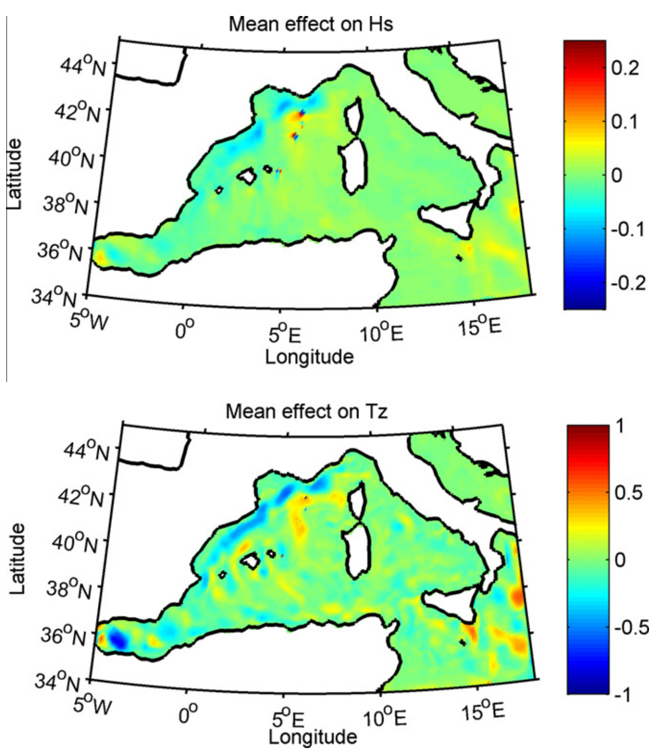

Fig. 13. Effect of currents on Hs (top panel) and mean period (bottom panel).

validation purposes an improvement of the boundaries will be required, but probably a ''simple'' extension of the domain will avoid this problem. From the tests done it seems that the boundaries have some local effect but they do not produce any large inconsistent values and the inner part of the domain does not seem to be affected. Therefore, for a sensitivity analysis they are considered to be appropriate.

5.4. Wave effects

Even though wave effects may be one of the processes lacking in ocean models, the present work showed that their effects are of second order compared to others. The main effect was an ''indirect'' one due to the modified wind stress which is equivalent to modification of wind velocities in an ocean model. This could also be assessed by comparison of this effect in an ensemble of wind fields considering a typical wind model error (Mitchell and Houtekamer, 2002; Mourre and Ballabrera-Poy, 2009). Wind stress is proportional to u^2 or u^3 (with a wind dependent drag), so a small error in the wind will produce a larger error in stress. The consideration of the surface stress partitioning delays the mixing at the beginning of the storm period. Waves are most of the time under development (not in balance with the wind), thus, the stress for currents (τ_c) is reduced and therefore velocities are reduced. Wave effects on surface currents were in the order of 5–15% the thermohaline circulation.

For the NW Mediterranean (a mostly deep area) the Stokes drift slightly modifies the surface currents and this has an impact on the distribution of temperature and salinity. Here, we have to point out that we are missing the direct effect of waves on turbulence (other than the Craig and Banner (1994)). In the present application, the direct wind effect alone is able to penetrate deep in the water column, and thus the wave effect is relatively minimized. This might be an artefact of the parameterisations that implicitly take into account the wave effects.

Another wave effect that could be considered is the radiation stress. Longuet-Higgins and Stewart (1962, 1964) described the radiation stress of surface waves as an excess flux of momentum due to the waves. Therefore momentum conservation modifies the current field induced by changes in the radiation stress. Its effects are more evident in shallow water due to wave momentum gradients caused by dissipation. Mellor (2003, 2005) derived the equations for the vertical distribution or radiation stress. Ardhuin et al. (2007) showed some inconsistency in such derivations mainly due to the assumptions of a flat bottom and Airy waves which lead to non-conservation of momentum and an error in the vertical momentum balance. Mellor (2008) addressed this problem and a modification of the radiation stress was performed. However, even the latest derivation is still controversial (Bennis and Ardhuin, 2010) and there is not a clear and well accepted formulation for the vertical distribution of radiation stress. For the NW Mediterranean this process is expected to be small except in areas of large wave gradients (eg. shallow coastal areas) where a 2D version of radiation stress could be used.

Acknowledgments

The authors thank the EU Marie-Curie project MARIE (MTKD-CT-2004-014509). Authors also thank Dr. F. Ardhuin at SHOM for valuable discussions during the development stage of the POLCOMS–WAM model. We acknowledge the support of Dr. S. Wakelin and Dr. C. Postlethwaite at POL during the implementation of POLCOMS. Thanks also to two anonymous referees for comments leading to significant improvements to the paper.

References

Ahumada, M.A., Cruzado, A., 2007. Modeling of the circulation in the Northwestern Mediterranean Sea with the Princeton Ocean Model. Ocean Science 3, 77–89.
Andrews, D.G., McIntyre, M.E., 1978a. An exact theory of nonlinear waves on a Lagrangian mean flow. Journal of Fluid Mechanics 89, 609–646.
Andrews, D.G., McIntyre, M.E., 1978b. On wave action and its relatives. Journal of Fluid Mechanics 89, 647–664.
Ardhuin, F., Jenkins, A.D., Belibassakis, K.A., 2007. Commentary on "The three dimensional current and surface wave equations" by George Mellor. Journal of Physical Oceanography, JPO-3670.
Ardhuin, F., Marie, L., Rascle, N., Forget, P., Roland, A., 2009. Observation and estimation of Lagrangian, Stokes, and Eulerian currents induced by wind and waves at the sea surface. Journal of Physical Oceanography 39 (11), 2820–2838.
Ardhuin, F., Rascle, N., Belibassakis, K.A., 2008. Explicit wave-averaged primitive equations using a generalized Lagrangian mean. Ocean Modelling 20, 35–60.
Ashworth, M., Holt, J.T., Proctor, R., 2004. Optimization of the POLCOMS hydrodynamic code for terascale high-performance computers. In: 18th International Parallel and Distributed Processing Symposium, Santa Fe, New Mexico. USA.
Babanin, A.V., 2006. On a wave-induced turbulence and a wave-mixed upper ocean layer. Geophysical Research Letters 33 (L20605).
Babanin, A.V., Ganopolski, A., Phillips, W.R.C., 2009. Wave-induced upper-ocean mixing in a climate model of intermediate complexity. Ocean Modelling 29 (3), 189–197.
Bargagli, A. et al., 2002. An integrated forecast system over the Mediterranean basin: extreme surge predictions in the northern Adriatic Sea. Monthly Weather Review 130 (5), 1317–1332.
Bennis, A.C., Ardhuin, F., in press. On the vertical structure of wave forcing for ocean circulation. <http://hal.archives-ouvertes.fr/docs/00/46/06/69/PDF/Bennis_Ardhuin_JPO2011_final_HAL.pdf>.
Blayo, E., Debreu, L., 2005. Revisiting open boundary conditions from the point of view of characteristics variables. Ocean Modelling 9, 231–252.
Blumberg, A., Mellor, G., 1987. A description of a three-dimensional coastal ocean circulation model. In: Heaps, N.S. (Ed.), Three-Dimensional Coastal Ocean Models, Coastal Estuarine Science. American Geophysical Union, pp. 1–16.
Bolaños, R., Sanchez-Arcilla, A., Cateura, J., 2007. Evaluation of two atmospheric models for wind–wave modelling in the NW Mediterranean. Journal of Marine Systems 65, 336–353.
Bolaños, R., Sanchez-Arcilla, A., Gomez, J., Cateura, J., Sairouni, A., 2004. Limits of operational wave prediction in the North-western Mediterranean, In: International Conference on Coastal Engineering, Lisbon, Portugal.
Brasseur, P., Beckers, J.M., Brankart, J.M., Schoenauen, R., 1996. Seasonal temperature and salinity fields in the Mediterranean Sea: climatological analysis of an historical data set. Deep-Sea Research 43, 159–192.
Broche, P., Forget, P., 1992. Has the influence of surface waves on wind stress to be accounted for in modelling the coastal circulation? Estuarine, Coastal and Shelf Science 35 (4), 347–351.
Brown, J.M., Wolf, J., 2009. Coupled wave and surge modelling for the eastern Irish Sea and implications for model wind-stress. Continental Shelf Research 29, 1329–1342.
Cavaleri, L., 2005. The wind and wave atlas of the Mediterranean Sea – the calibration phase. Advances in Geoscience 2, 255–257.
Cavaleri, L., Bertotti, L., 2004. The accuracy of modelled wind and wave fields in enclosed seas. Tellus 56A, 167–175.
Cavaleri, L., Sclavo, M., 2006. The calibration of wind and wave model data in the Mediterranean Sea. Coastal Engineering 53, 613–627.
Codina, B., Aran, M., Young, S., Redano, A., 1997. Prediction of a mesoscale convective system over the Catalonia (North-eastern Spain) with a nested numerical model. Atmospheric Physics 62, 9–22.
Conan, P., Millot, C., 1995. Variability of the Northern current off Marseilles, western Mediterranean Sea, from February to June 1992. Oceanology Acta 18 (2), 193–205.
Craig, P.D., Banner, M.L., 1994. Modeling wave-enhanced turbulence in the ocean surface layer. Journal of Physical Oceanography 24, 2546–2559.
Feddersen, F., 2004. Effect of wave directional spread on the radiation stress: comparing theory and observations. Coastal Engineering 51, 473–481.
Flamant, C.V. et al., 2003. Analysis of surface wind and roughness length evolution with fetch using a combination of airborne lidar and radar measurements. Journal of Geophysical Research 108 (C3), 26.
Flexas, M.M., Durrieu de Madron, X., Garcia, M.A., Canals, M., Arnau, P., 2002. Flow variability in the Gulf of Lions during the Mater HFF Experiment (March–May 1997). Journal of Marine Systems, 197–214.
Font, J., 1990. A comparison of seasonal winds with currents on the continental slope of the Catalan Sea (Northwestern Mediterranean). Journal of Geophysical Research 95 (C2), 1537–1545.
Gemmrich, J.R., Farmer, D.M., 2004. Near-surface turbulence in the presence of breaking waves. Journal of Physical Oceanography 34, 1067–1086.
Groeneweg, J., Battjes, J.A., 2003. Three dimensional wave effects on a steady current. Journal of Fluid Mechanics 478, 325–343.
Hasselman, K., 1970. Wave-driven inertial oscillations. Geophysical Fluid Dynamics 1, 463–502.
Holt, J.T., James, I.D., 1999. A simulation of the southern North Sea in comparison with measurements from the North Sea Project. Part 1: Temperature. Continental Shelf Research 19, 1087–1112.
Holt, J.T., James, I.D., 2001. An S coordinate density evolving model for the northwest European continental shelf. Model description and density structure. Journal of Geophysical Research 106 (C7), 14015–14034.
Holt, J.T., Umlauf, L., 2008. Modelling the tidal mixing fronts on seasonal stratification of the Northwest European continental shelf. Continental Shelf Research 28, 887–903.
Janssen, P.A.E.M., 1989. Wave-induced stress and the drag of air flow over the sea waves. Journal of Physical Oceanography 19, 745–754.
Janssen, P.A.E.M., 1991. Quasi-linear theory of wind generation applied to wave forecasting. Journal of Physical Oceanography 21, 1631–1642.
Janssen, P.A.E.M., Saetra, O., Wettre, C., Hersbach, H., Bidlot, J., 2004. The impact of the sea state on the atmosphere and oceans. Annales Hydrographiques 3 (772), 3.1–3.23.
Jenkins, A.D., 1987. Wind and wave induced currents in a rotating sea with depth-varying eddy viscosity. Journal of Physical Oceanography 17, 938–951.
Jorda, G., 2005. Towards data assimilation in the Catalan continental shelf. From data analysis to optimization methods, Universidad Politecnica de Catalunya, 332 pp.
Jorda, G., Bolanos, R., Espino, M., Sanchez-Arcilla, A., 2007. Assessment of the importance of the current-wave coupling in the shelf ocean forecast. Ocean Science 3, 345–362.
Kirby, J.T., Chen, T.M., 1989. Surface waves on vertically sheared flows: approximate dispersion relations. Journal of Geophysical Research 94 (C1), 1013–1027.
Komen, G.J., Cavaleri, L., Donelan, M., Hasselman, K., Hasselman, S., Janssen, P.A.E.M., 1994. Dynamics and Modelling of Ocean Waves. Cambridge University Press. 532 pp..
Komen, G.J., Hasselmann, S., Hasselman, K., 1984. On the existence of a fully developed wind-sea spectrum. Journal of Physical Oceanography 14, 1271–1285.
Krivtsov, V., Howarth, M.J., Jones, S.E., Souza, A.J., Jago, C.F., 2008. Monitoring and modelling of the Irish Sea and Liverpool Bay: an overview and an SPM case study. Ecological Modelling 212, 37–52.
Lane, E.M., Restrepo, J.M., McWilliams, J.C., 2007. Wave-current interaction: a comparison of radiation-stress and vortex-force representation. Journal of Physical Oceanography 37 (5), 1122–1141.
Lavelle, J.W., Thacker, W.C., 2008. A pretty good sponge: dealing with open boundaries in limited-area ocean models. Ocean Modelling 20, 270–292.
Lewis, D.M., Belcher, S.E., 2004. Time-dependent, coupled, Ekman boundary layer solutions incorporating Stokes drift. Dynamics of Atmospheres and Oceans 37, 313–351.
Longo, S., Petti, M., Losada, I.J., 2002. Turbulence in the swash and surf zones: a review. Coastal Engineering 45, 129–147.
Longuet-Higgins, M.S., Stewart, R.W., 1962. Radiation stress and mass transport in gravity waves with applications to surf 'beats'. Journal of Fluid Mechanics 13, 481–504.
Longuet-Higgins, M.S., Stewart, R.W., 1964. Radiation stress in water waves: a physical discussion with applications. Deep-Sea Research 11, 529–562.
Madsen, O.S., 1994. Spectral wave-current bottom boundary layers flow, ICCE, pp. 384–398.
Makin, V.K., Kudryavtsev, V.N., 1999. Coupled sea surface-atmosphere model 1. Wind over waves coupling. Journal of Geophysical Research 104, 7613–7623.
Makin, V.K., Kudryavtsev, V.N., 2002. Impact of dominant waves on sea drag. Boundary-layer Meteorology 103, 83–99.
Marsaleix, P., Estournel, C., Kondrachoff, V., Vehil, R., 1998. A numerical study of the formation of the Rhone river plume. Journal of Marine Systems 14, 99–115.
McWilliams, J.C., Restrepo, J.M., Lane, E.M., 2004. An asymptotic theory for the interaction of waves and currents in coastal waters. Journal of Fluid Mechanics 511, 135–178.

Mellor, G., 2003. The three-dimensional current and surface wave equations. Journal of Physical Oceanography 33, 1978–1989.
Mellor, G., 2005. Some consequences of the three-dimensional current and surface wave equations. Journal of Physical Oceanography 35, 2291–2298.
Mellor, G., 2008. The depth-dependent current and wave interaction equations: a revision. Journal of Physical Oceanography 38, 2587–2596.
Mellor, G., Blumberg, A., 2004. Wave breaking and ocean surface layer thermal response. Journal of Physical Oceanography 34 (Notes and correspondence), 693–694.
Mellor, G., Yamada, T., 1974. A hierarchy of turbulence closure models for planetary boundary layers. Journal of Atmospheric Science 31, 1791–1806.
Mellor, G., Yamada, T., 1982. Development of a turbulence closure model for geophysical fluid problems. Rev. Geophys. 20, 851–875.
MESO, 1994. MASS version 5.6 Reference Manual, NY.
Millot, C., 1999. Circulation in the Western Mediterranean Sea. Journal of Marine Systems 20, 423–442.
Mitchell, H.L., Houtekamer, P.L., 2002. Ensemble size, balance and model-error representation in an ensemble Kalman filter. Monthly Weather Review 130 (11), 2791–2808.
Monbaliu, J. et al., 2000. The spectral wave model, WAM, adapted for applications with high spatial resolution. Coastal Engineering 41 (1–3), 41–62.
Moore, R.D., Wolf, J., Souza, A.J., Flint, S.S., 2009. Morphological evolution of the Dee Estuary, Eastern Irish sea, UK: a tidal asymmetry approach. Geomorphology 103, 588–596.
Mourre, B., Ballabrera-Poy, J., 2009. Salinity model errors induced by wind stress uncertainties in the Macaronesian region. Ocean Modelling 29 (3), 213–221.
Munich-Reinsurance-Company, 2004. Annual Report.
Osuna, P., Wolf, J., 2005. A numerical study of the effect of wave–current interaction processes in the hydrodynamics of the Irish Sea. In: International Conference on ocean Waves and Analysis. WAVES., Madrid, Spain.
Ozer, J. et al., 2000. A coupling module for tides, surges and waves. Coastal Engineering 41 (1–3), 95–124.
Pinardi, N., Masetti, E., 2000. Variability of the large-scale general circulation of the Mediterranean Sea from observations and modelling: a review. Palaeogeography, Palaeoclimatology, Palaeoecology 158, 153–173.
Pinardi, N., Woods, J., 2002. Ocean Forecasting. Conceptual Basis and Applications. Springer.
Pizzigalli, C., Rupolo, V., Lombardi, E., Blanke, B., 2007. Seasonal probability dispersion maps in the Mediterranean Sea obtained from the Mediterranean Forcasting System Eulerian velocity fields. Journal of Geophysical Research 112 (C05012).
Polton, J.A., Lewis, D.M., Belcher, S.E., 2005. The role of the wave-induced Coriolis–Stokes forcing on the wind-driven mixed layer. Journal of Physical Oceanography 35 (4), 444–457.
Proctor, R., James, I.D., 1996. A fine-resolution 3D model of the southern North Sea. Journal of Marine Systems 8, 131–146.
Qiao, F. et al., 2004. Wave-induced mixing in the upper ocean: distribution and application to a global ocean circulation model. Geophysical Research Letters 31, L11303.
Rascle, N., Ardhuin, F., 2009. Drift and mixing under the ocean surface revisited: stratified conditions and model-data comparisons. Journal of Geophysical Research 114 (C02016).
Rascle, N., Ardhuin, F., Terray, E.A., 2006. Drift and mixing under the ocean surface: a coherent one-dimensional description with application to unstratified conditions. Journal of Geophysical Research 111 (C3).
Ratsimandresy, A.W., Sotillo, M.G., Carretero, J.C., Alvarez Fanjul, E., Hajji, H., 2008. A 44-year high-resolution ocean and atmospheric hindcast for the Mediterranean Basin developed within the HIPOCAS project. Coastal Engineering 55 (11), 827–842.
Rippeth, T.P., Simpson, J.H., Player, R.J., Garcia, M., 2002. Current oscillations in the diurnal-inertial band on the Catalonian shelf in spring. Continental Shelf Research 22, 247–265.
Rodriguez, J. et al., 2001. The role of mesoscale vertical motion in controlling the size structure of phytoplankton in the ocean. Nature 410, 360–363.
Roland, A. et al., 2009. On the development and verification of a 2-D coupled wave–current model on unstructured meshes. Journal of Marine Systems. doi:10.1016?j.jmarsys.2009.01.026.
Rubio, A. et al., 2005. A field study of the behaviour of an anticyclonic eddy on the Catalan continental shelf (NW Mediterranean). Progress in Oceanography 66 (2–4), 142–156.
Rubio, A. et al., 2009. Origin and dynamics of mesoscale eddies in the Catalan Sea (NW Mediterranean): Insight from a numerical model study. Journal of Geophysical Research 114 (C06009).
Sabates, A., Salat, J., Maso, M., 2004. Spatial heterogeneity of fish larvae across a meandering in the northwestern Mediterranean. Deep-Sea Research II 51, 545–557.
Siddorn, J.R. et al., 2007. Modelling the hydrodynamics and ecosystem of the North-West European continental shelf for operational oceanography. Journal of Marine Systems 65, 417–429.
Smith, J.A., 2006. Observed variability of ocean wave Stokes drift and the Eulerian response to passing groups. Journal of Physical Oceanography 36, 1381–1402.
Smith, S.D., Banke, E.G., 1975. Variation of the sea surface drag coefficient with wind speed. Quarterly Journal of the Royal Meteorological Society 101, 665–673.
Tang, C.L. et al., 2007. Observation and modelling of surface currents on the Grand Banks: a study of the wave effects on surface currents. Journal of Geophysical Research 113 (C10025).
van der Westhuysen, A.J., Zijlema, M., Battjes, J.A., 2007. Nonlinear saturation-based whitecapping dissipation in SWAN for deep and shallow water. Coastal Engineering 54 (2), 151–170.
Wakelin, S.L., Holt, J.T., Proctor, R., 2009. The influence of initial conditions and open boundary conditions on shelf circulation in a 3D ocean-shelf model of the North East Atlantic. Ocean Dynamics 59, 67–81.
WAMDI-Group, 1988. The WAM model – a third generation ocean wave prediction model. Journal of Physical Oceanography 18, 1775–1810.
Weber, J.E.H., Brostrom, G., Saetra, O., 2006. Eulerian versus Lagrangian approaches to the wave-induced transport in the upper ocean. Journal of Physical Oceanography 31 (11), 2106–2118.
Wolf, J., 2009. Coastal flooding – impact of coupled wave–surge models. Natural Hazards 49 (2), 241–260.
Wu, P., Haines, K., Pinardi, N., 2000. Toward an understanding of deep-water renewal in the Eastern Mediterranean. Journal of Physical Oceanography 30, 443–458.
Xu, Z., Bowen, A.J., 1994. Wave and wind-driven flow in water of finite depth. Journal of Physical Oceanography 24, 1850–1866.
Yu, J., Slinn, D.N., 2003. Effect of wave–current interaction on rip currents. Journal of Geophysical Research 108, 3088.